

INFLUENCE OF SORET AND DUFOUR EFFECTS ON UNSTEADY HEAT AND MASS TRANSFER FLOW OF A MICROPOLAR FLUID WITH HEAT SOURCES

S VENKATA RAMI REDDY

Dept of Mathematics, BT College , Madanapalle , AP , India.

ABSTRACT

The combined influence of Heat source, Soret and Dufour effects on transient convective heat and mass transfer flow of a micro polar fluid through porous medium. The non linear coupled equations governing the flow heat and mass transfer flow have been solved by Employing Galerkin in finite element technique with quadratic approximation polynomials. The velocity, micro rotation, temperature and concentration have been discussed for governing parameters. The skin friction, the rate of heat and mass transfer have evaluated numerically for different parametric variations.

KEYWORDS : Heat and Mass Transfer, Soret and Dufour Effects, Finite Element Technique , Micro Polar Fluid.

1. INTRODUCTION

The boundary layer flow, heat and mass transfer in a quiescent Newtonian and non-Newtonian fluid driven by a continuous stretching sheet are of significance in a number of industrial engineering processes such as drawing of a polymer sheet or filaments extruded continuously from a die , the cooling of a metallic plate in a bath, the aerodynamic extrusion of plastic sheets, the continuous casting, rolling, annealing and thinning of copper wires, the wires are fiber coating etc .The final product of desired characteristics depends on the rate of cooling in the process and the process of stretching. Mohammadi and Nourazar [16] studied on the insertion of a thin gas layer in micro cylindrical coquette flows involving power-law liquids. The analytical solution for two- phase flow between two rotating cylinders filled with power-law liquid and a micro layer of gas has been investigated by Mohammadi et al [17]. The dynamics of the boundary layer flow over a

stretching surface originated from the pioneering work of carne [6]. Srinivasacharya et al [21] analyzed the unsteady flow of micro polar fluid between two parallel porous plates. Bhargava et al [2] investigated by using a finite element method the flow of a mixed convection micro polar fluid driven by a porous stretching sheet with uniform suction.

Ali and Magyari [1] have studied the unsteady fluid and heat flow by a submerged stretching surface while its steady motion is slowed down gradually. Mukhopadhyay [18] extended it by assuming the viscosity and thermal diffusivity are linear functions of temperature and studied unsteady mixed convection boundary layer flow of an incompressible viscous liquid through porous medium along a permeable surface, and the thermal radiation effect on heat transfer was also considered.

Mohamood and Nadeem et al. [15] have been analyzed the heat transfer analysis of water-based nanofluid over an exponentially stretching sheet. The nano fluid flow over an unsteady stretching surface in the presence of thermal radiation was examined by Das et al.[7]. The fluid flow past over a stretching sheet has been studied by many authors. Yacos et al [27] have been investigated melting heat transfer in boundary layer stagnation point flow towards a stretching/shrinking sheet in micro polar fluid. Mahmood et al.[14] analyzed the non-orthogonal stagnation point flow of a micro polar second-grade fluid toward a stretching/shrinking sheet in a porous medium with suction was observed by Rosali et al.[20]. Heat and Mass transfer on MHD flow of a visco elastic fluid through porous medium over a shrinking sheet was investigated by Bhukta et al [3]. Mahmood and Waheed [14] have been proposed the MHD flow and heat transfer of a micro polar fluid over a stretching surface with heat generation (absorption) and slip velocity. The boundary layer flow of hyperbolic tangent fluid over a vertical exponentially stretching cylinder was studied by Ishak and Nazar et al. [9].

As many industrially and environmentally relevant fluids are not pure, it is been suggested that more attention should be paid to convective phenomena which can occur in mixtures, but are not in common liquids such as air or water. Applications involving liquid mixtures include the costing of alloys, ground water pollutant migration and separation operations. In all of these situations, multi component liquids can undergo natural

convection driven by buoyancy force resulting from simultaneous temperature and species gradients. In the case of binary mixtures, the species gradients can be established by the applied boundary conditions such as species rejection associated with alloys costing, or can be induced by transport mechanism such as Soret (thermo) diffusion. In the case of Soret diffusion, species gradients are established in an otherwise uniform concentration mixture in accordance with an inverse relationship. Thermal-diffusion known as the Soret effect takes place and as a result a mass fraction distribution is established in the liquid layer. The sense of migration of the molecular species is determined by the sign of Soret coefficient. Soret and Dufour effects are very significant in both Newtonian and non-Newtonian fluids when density differences exist in flow regime. The thermo-diffusion (Soret) effect corresponds to species differentiation developing in an initial homogeneous mixture submitted to a thermal gradient and the diffusion-thermo (Dufour) effect corresponds to the heat flux produced by a concentration gradient. Usually, in heat and mass transfer problems the variation of density with temperature and concentration give rise to a combined buoyancy force under natural convection and hence the temperature and concentration will influence the diffusion and energy of the species. Many papers are found in literature on Soret and Dufour effects on different geometries. Reddy et al. [19] has presented finite element solution to the heat and mass transfer flow past a cylindrical annulus with Soret and Dufour effects. Recently, Chamkha et al. [4] has studied the influence of Soret and Dufour effects on unsteady heat and mass transfer flow over a rotating vertical cone and they suggested that temperature and concentration fields are more influenced with the values of Soret and Dufour parameter.

Wang [26] was first studied the unsteady boundary layer flow of a liquid film over a stretching sheet. Later, Elbashbeshy and Bazid [8] have presented the heat transfer over an unsteady stretching surface. Tsai et al. [24] has discussed flow and heat transfer characteristics over an unsteady stretching surface by taking heat source into the account. Ishak et al [9] analyzed the effect of prescribed wall temperature on heat transfer flow over an unsteady stretching permeable surface.

In this chapter, we investigate the combined influence of Heat source, Soret and Dufour effects on transient convective heat and mass transfer flow of a micro polar fluid

through porous medium. The non linear coupled equations governing the flow heat and mass transfer flow have been solved by Employing Galerkin finite element technique with quadratic approximation polynomials. The velocity, micro rotation, temperature and concentration have been discussed for governing parameters. The skin friction, the rate of heat and mass transfer have evaluated numerically for different parametric variations.

2. FORMULATION OF THE PROBLEM

We analyse two-dimensional transient unsteady viscous electrically conducting heat and mass transfer of micro polar fluid flow through porous medium over a stretching sheet in the presence of suction/injection, Soret and Dufour effects in slip flow regime. The coordinate system is such that x -axis is taken along the stretching surface in the direction of the motion with the slot at origin and the y -axis is perpendicular to the surface of the sheet as shown schematically in Fig.1. A uniform transverse magnetic field (B_0) is applied along the y -axis. The stretching surface and the fluid are maintained same temperature and concentration initially, instantaneously they raised to a temperature $T_w (> T_\infty)$ and concentration $C_w (> C_\infty)$ which remain unchanged. Under the above stated physical situations, the governing boundary-layer and Darcy-Boussinesq's approximations, the basic equations are given by:

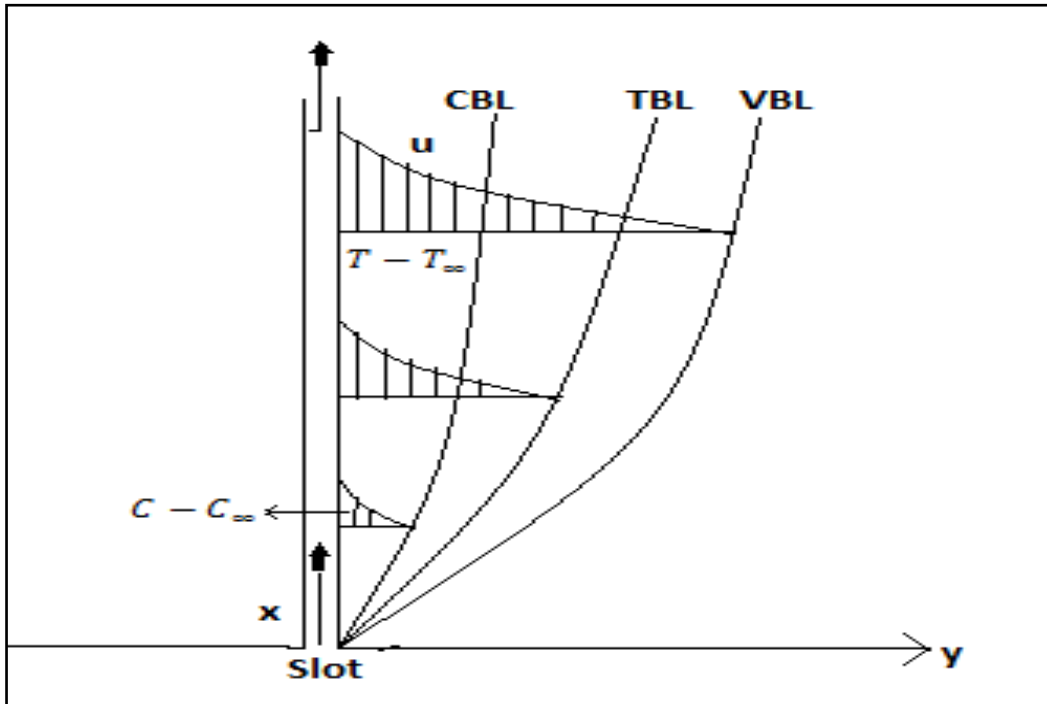


Fig. 1. Flow configuration and coordinate system.

(2.1)

$$\frac{\partial u}{\partial t} + u \frac{\partial u}{\partial x} + v \frac{\partial u}{\partial y} = (v + \frac{k_1}{\rho}) \frac{\partial^2 u}{\partial y^2} + k \frac{\partial \omega}{\partial y} + g(\beta(T - T_\infty) + \beta^\infty(C - C_\infty)) - (\frac{\mu}{\rho k})u - \frac{\sigma B_o^2}{\rho}u \quad (2.2)$$

$$\frac{\partial \omega}{\partial t} + u \frac{\partial \omega}{\partial x} + v \frac{\partial \omega}{\partial y} = (\frac{\gamma}{\rho j}) \frac{\partial^2 \omega}{\partial y^2} + (\frac{k_1}{\rho j})(2\omega + \frac{\partial u}{\partial y}) \quad (2.3)$$

$$\frac{\partial T}{\partial t} + u \frac{\partial T}{\partial x} + v \frac{\partial T}{\partial y} = (\frac{k_f}{\rho C_p}) \frac{\partial^2 T}{\partial y^2} + (\frac{\mu}{\rho C_p})(\frac{\partial u}{\partial y})^2 + (\frac{D_T K_T}{C_s C_p}) \frac{\partial^2 C}{\partial y^2} - Q_H(T - T_\infty) \quad (2.4)$$

$$\frac{\partial C}{\partial t} + u \frac{\partial C}{\partial x} + v \frac{\partial C}{\partial y} = (D_m) \frac{\partial^2 C}{\partial y^2} + \left(\frac{D_m K_T}{T_m}\right) \frac{\partial^2 T}{\partial y^2} \quad (2.5)$$

The associated boundary conditions on the vertical surface are defined as follows

$$U = U_w = ax, v = -v_w, \frac{\partial T}{\partial y} = -\frac{q_w}{k_f}, \frac{\partial C}{\partial y} = -\frac{m_w}{D_m}, \omega' = 0 \quad \text{at } y = 0$$

$$U \rightarrow 0, T \rightarrow T_\infty, C \rightarrow C_\infty, \omega' = 0 \quad \text{at } y \rightarrow \infty \quad (2.6)$$

The boundary condition $\omega = 0$ at $y = 0$ in Eq. (5.2.6), represents the case of concentrated particle flows in which the microelements close to the wall are not able to rotate, due to the no slip condition in the above equations x and y represents coordinate axis along the continuous surface in the direction of motion and perpendicular to it, u and v are the velocity components along x and y directions, respectively. The term $V_w = -\sqrt{\frac{av}{2}}V_o$ represents the mass transfer at the surface with $V_w < 0$ for suction and $V_w > 0$ for injection.

The following similarity transformations are introduced to simplify the mathematical analysis of the problem

$$\eta = \sqrt{\frac{a}{v(1-ct)}}y, \psi = \sqrt{\frac{av}{(1-ct)}}f(\eta), u = \frac{ax}{(1-ct)}, v = -\sqrt{\frac{av}{(1-ct)}}f(\eta) \quad (2.7)$$

$$T = T_\infty + \frac{bx}{(1-ct)^2}, C = C_\infty + \frac{dx}{(1-ct)^2}$$

Using equation (2.7), the governing equations (2.2) – (2.5) are transformed into the following form

$$(1 + A1)f''' + ff'' - (f')^2 - A(f' + \frac{1}{2}\eta f'') + A1g' + G(\theta + N\phi) - (M^2 + D^{-1})f' = 0 \quad (2.8)$$

$$\lambda g'' + fg' - gf' - \frac{A}{2}(3g + \eta g') + A1B(2g + f'') = 0 \tag{2.9}$$

$$\theta'' + Pr(f\theta' - f'\theta) - Pr \frac{A}{2}(4\theta + \eta\theta') - Ec(f'')^2 + Du\phi'' - Q\theta = 0 \tag{2.10}$$

$$\phi'' - Sc(f\phi\theta - f'\phi) - Sc \frac{A}{2}(4\phi + \eta\phi\theta) + ScSr\theta\phi = 0 \tag{2.11}$$

The corresponding transformed boundary conditions are

$$f' = 1, f = fw, g = 0, \frac{\partial \theta}{\partial y} = -1, \frac{\partial \phi}{\partial y} = -1, \omega = 0 \text{ at } \eta = 0$$

$$f' = 0, g = 0, \theta = 0, \phi = 0 \text{ as } \eta \rightarrow \infty$$

$$f' = 0, \quad g = 0, \quad \theta = 0, \quad \phi = 0, \quad \text{at } y \rightarrow \infty \tag{2.12}$$

where

$$A1 = \frac{\mu}{k} \text{ (coupling paramete)}, G = \frac{\beta g(T_w - T_\infty)}{a^2} \text{ (Grashof number)}$$

$$N = \frac{\beta^*(C_w - C_\infty)}{\beta(T_w - T_\infty)} \text{ (buoyancy parameter)}, A = \frac{c}{a} \text{ (unsteadiness parameter)}$$

$$D^{-1} = \frac{v(1-ct)}{ka} \text{ (Inverse Darcy parameter)}, Pr = \frac{\mu C}{k_f} \text{ (Pr andtlparaameter)}$$

$$Sc = \frac{v}{D_m} \text{ (Schmidt parameter)}, Sr = \frac{D_m K_T}{v T_m} \text{ (Soret parameter)}$$

$$Du = \frac{D_m K_T l}{C_s C_p b v} \text{ (Dufour parameter)}, Ec = \frac{a^2 x}{C_p b} \text{ (Ec ker tNumber)}$$

$$M = \frac{\sigma B_o^2 (1-ct)}{\rho a} \text{ (Magnetic parameter)}$$

$$\lambda_0 = \frac{\nu}{\nu j}, B = \frac{\nu(1-ct)}{aj}$$

The major physical quantities of interest in this problem are the local skin friction coefficient (C_{fx}), couple stress coefficient (C_{sx}), local Nusselt number (Nu_x) and the local Sherwood number (Sh_x) are defined, respectively, by

$$C_{fx} = \frac{2(1+Al)f''(0)}{R_{ex}^{1/2}}, C_{sx} = \frac{\nu a U_w h'(0)}{R_{ex}^{1/2}}, Nu_x = -\frac{1}{R_{ex}^{1/2}} \left(\frac{1}{\theta(0)} \right), Sh_x = -\frac{1}{R_{ex}^{1/2}} \left(\frac{1}{\phi(0)} \right)$$

3. SOLUTION OF THE PROBLEM

The set of ordinary differential equations (2.8) – (2.11) are highly non-linear, and therefore cannot be solved analytically. The Finite-element method has been employed to solve these non-linear equations. The procedure of Finite element method is as follows.

- (i) Finite-element discretization
- (ii) Generation of the element equations
- (iii) Assembly of element equations
- (iv) Imposition of boundary conditions
- (v) Solution of assembled equations

The very important aspect in this numerical procedure is to select an approximate finite value. So in order to estimate the relevant value of the solution process has been started with an initial value of and then the equations (2.8) – (2.11) are solved together with boundary conditions (2.12). We have updated the value of and the solution process is continued until the results are not affected with further values of the choice for velocity, for micro-rotation, for temperature and for concentration have confirmed that all the numerical solutions approach to the asymptotic values at the free stream conditions.

For the solution of system of non-linear ordinary differential equation (2.8) – (2.11) together with boundary conditions (2.12), first we assume that

$$\frac{\partial f}{\partial \eta} = j \tag{3.1}$$

The equations (2.8) to (2.11) then reduces to

$$(1 + A1)j'' + ff' - (j)^2 - A(j + \frac{1}{2}\eta j') + A1g' + G(\theta + N\phi) - (M^2 + D^{-1})j = 0 \tag{3.2}$$

$$\lambda g'' + fg' - gf' - \frac{A}{2}(3g + \eta g') + A1B(2g + j') = 0 \tag{3.3}$$

$$\theta'' + Pr(f\theta' - j\theta) - Pr\frac{A}{2}(4\theta + \eta\theta') - Ec(j')^2 + Du\phi'' - Q\theta = 0 \tag{3.4}$$

$$\phi'' - Sc(f\phi\theta - j\phi) - Sc\frac{A}{2}(4\phi + \eta\phi') + ScSr\theta'' = 0 \tag{3.5}$$

The boundary conditions take the form

$$\begin{aligned} j = 1, f = fw, g = 0, \frac{d\theta}{d\eta} = -1, \frac{d\phi}{d\eta} = -1 \text{ at } \eta = 0 \\ j = 0, g = 0, \theta = 0, \phi = 0 \text{ as } \eta \rightarrow \infty \end{aligned} \tag{3.6}$$

Variational formulation

The variational form associated with Eqs. (20) to (24) over a typical linear element (η_e, η_{e+1}) is given by

$$\int_{\eta_e}^{\eta_{e+1}} w_1 \left(\frac{\partial f}{\partial \eta} - j \right) d\eta = 0 \tag{3.7}$$

$$\int_{\eta_e}^{\eta_{e+1}} w_2((1 + A1)f''' + ff'' - (f')^2 - A(f' + \frac{1}{2}\eta f'') + A1g' + G(\theta + N\phi) - (M^2 + D^{-1})f')d\eta = 0 \tag{3.8}$$

$$\int_{\eta_e}^{\eta_{e+1}} w_2(\lambda g'' + fg' - gf' - \frac{A}{2}(3g + \eta g') + A1B(2g + j') = 0)d\eta = 0 \tag{3.0}$$

(5.3.8)

$$\tag{3.11}$$

$$\int_{\eta_e}^{\eta_{e+1}} w_4(\theta'' + Pr(f\theta' - j\theta) - Pr \frac{A}{2}(4\theta + \eta\theta') - Ec(j')^2 + Du\phi'' - Q\theta)d\eta = 0$$

$$\int_{\eta_e}^{\eta_{e+1}} w_5(\phi'' - Sc(f\phi' - j\phi) - Sc \frac{A}{2}(4\phi + \eta\phi') + ScSr\theta'')d\eta = 0$$

$$\tag{3.11}$$

Where w_1, w_2, w_3, w_4, w_5 are arbitrary test functions and may be viewed as the variations in $f, j, g, \theta,$ and $\phi,$ respectively.

(vii) Finite- element formulation

The finite-element model may be obtained from above equations by substituting finite-element approximations of the form

$$f = \sum_{j=1}^3 f_j \psi_j, j = \sum_{j=1}^3 j_j \psi_j, g = \sum_{j=1}^3 g_j \psi_j, \theta = \sum_{j=1}^3 \theta_j \psi_j, \phi = \sum_{j=1}^3 \phi_j \psi_j$$

With $w_1=w_2=w_3=w_4=w_5 = \psi_j (i=1,2,3)$

Where ψ_j are the shape functions for a typical element (η_e, η_{e+1}) and are defined as

$$\psi_1^e = \frac{(\eta_{e+1} + \eta_e - 2\eta)(\eta_{e+1} - \eta)}{(\eta_{e+1} - \eta_e)^2}, \psi_3^e = \frac{(\eta_{e+1} + \eta_e - 2\eta)(\eta - \eta_{e+1})}{(\eta_{e+1} - \eta_e)^2}$$

$$\psi_2^e = \frac{4(\eta - \eta_e)(\eta_{e+1} - \eta)}{(\eta_{e+1} - \eta_e)^2} \quad (\eta_e \leq \eta \leq \eta_{e+1})$$

The finite element model of the equations thus formed is given by

$$\begin{bmatrix} [K^{11}] & [K^{12}] & [K^{13}] & [K^{14}] & [K^{15}] \\ [K^{21}] & [K^{22}] & [K^{23}] & [K^{24}] & [K^{25}] \\ [K^{31}] & [K^{32}] & [K^{33}] & [K^{34}] & [K^{35}] \\ [K^{41}] & [K^{42}] & [K^{43}] & [K^{44}] & [K^{45}] \\ [K^{51}] & [K^{52}] & [K^{53}] & [K^{54}] & [K^{55}] \end{bmatrix} \begin{bmatrix} f \\ j \\ g \\ \theta \\ \phi \end{bmatrix} = \begin{bmatrix} \tau^1 \\ \tau^2 \\ \tau^3 \\ \tau^4 \\ \tau^5 \end{bmatrix}$$

where $[K^{mn}]$ and $[\tau^m]$ (m,n=1,2,3,4,5) are defined as

$$K_{ij}^{11} = \int_{\eta_e}^{\eta_{e+1}} \psi_i \frac{\partial \psi_j}{\partial \eta} d\eta, K_{ij}^{12} = -\int_{\eta_e}^{\eta_{e+1}} \psi_i \psi_j d\eta, K_{ij}^{13} = K_{ij}^{14} = K_{ij}^{15} = 0$$

$$K_{ij}^{41} = 0, K_{ij}^{42} = Ec \int_{\eta_e}^{\eta_{e+1}} \psi_i \psi_1 \left(\frac{\partial \psi_j}{\partial \eta}\right)^2 d\eta, K_{ij}^{43} = 0,$$

$$K_{ij}^{44} = -\int_{\eta_e}^{\eta_{e+1}} \frac{\partial \psi_i}{\partial \eta} \frac{\partial \psi_j}{\partial \eta} d\eta + Pr(1 + 1.5A\eta) \bar{f}_1 \int_{\eta_e}^{\eta_{e+1}} \psi_i \psi_1 \left(\frac{\partial \psi_j}{\partial \eta}\right) d\eta +$$

$$Pr(1 + 1.5A\eta) \bar{f}_2 \int_{\eta_e}^{\eta_{e+1}} \psi_i \psi_2 \left(\frac{\partial \psi_j}{\partial \eta}\right) d\eta + Pr(1 + Q + 1.5A\eta) \bar{j}_1 \int_{\eta_e}^{\eta_{e+1}} \psi_i \psi_1 \psi_j d\eta +$$

$$Pr(1 + Q + 1.5A\eta) \bar{j}_2 \int_{\eta_e}^{\eta_{e+1}} \psi_i \psi_2 \psi_j d\eta$$

$$\begin{aligned}
 K_{ij}^{23} &= A1\bar{g}_1 \int_{\eta_e}^{\eta_{e+1}} \psi_i \psi_1 \psi_j d\eta - A1\bar{g}_2 \int_{\eta_e}^{\eta_{e+1}} \psi_i \psi_2 \psi_j d\eta \\
 K_{ij}^{31} &= 0, K_{ij}^{32} = 0 \\
 K_{ij}^{33} &= -\lambda \int_{\eta_e}^{\eta_{e+1}} \frac{\partial \psi_i}{\partial \eta} \frac{\partial \psi_j}{\partial \eta} d\eta - (2A1B + 1.5A\bar{j}) \int_{\eta_e}^{\eta_{e+1}} \psi_i \psi_1 \psi_j d\eta + \\
 &1.5A\eta \int_{\eta_e}^{\eta_{e+1}} \psi_i \psi_1 \frac{\partial \psi_j}{\partial \eta} d\eta + 1.5A\eta \int_{\eta_e}^{\eta_{e+1}} \psi_i \psi_2 \frac{\partial \psi_j}{\partial \eta} d\eta, K_{ij}^{34} = K_{ij}^{35} = 0 \\
 K_{ij}^{22} &= -(1 + A1) \int_{\eta_e}^{\eta_{e+1}} \frac{\partial \psi_i}{\partial \eta} \frac{\partial \psi_j}{\partial \eta} d\eta - (M^2 + D^1) \int_{\eta_e}^{\eta_{e+1}} \psi_i \psi_j d\eta + \\
 &0.5A \int_{\eta_e}^{\eta_{e+1}} \psi_i \psi_1 \frac{\partial \psi_j}{\partial \eta} d\eta + 0.5A \int_{\eta_e}^{\eta_{e+1}} \psi_i \psi_2 \frac{\partial \psi_j}{\partial \eta} d\eta - \bar{f}_1 \int_{\eta_e}^{\eta_{e+1}} \psi_i \psi_1 \frac{\partial \psi_j}{\partial \eta} d\eta - \\
 &\bar{f}_2 \int_{\eta_e}^{\eta_{e+1}} \psi_i \psi_2 \frac{\partial \psi_j}{\partial \eta} d\eta \\
 K_{ij}^{45} &= -\int_{\eta_e}^{\eta_{e+1}} \frac{\partial \psi_i}{\partial \eta} \frac{\partial \psi_j}{\partial \eta} d\eta, K_{ij}^{51} = 0, K_{ij}^{52} = 0, K_{ij}^{53} = 0, \\
 K_{ij}^{54} &= -ScSr \int_{\eta_e}^{\eta_{e+1}} \frac{\partial \psi_i}{\partial \eta} \frac{\partial \psi_j}{\partial \eta} d\eta, \\
 K_{ij}^{55} &= -\int_{\eta_e}^{\eta_{e+1}} \frac{\partial \psi_i}{\partial \eta} \frac{\partial \psi_j}{\partial \eta} d\eta + Sc(1 + 1.5A\eta) \bar{f}_1 \int_{\eta_e}^{\eta_{e+1}} \psi_i \psi_1 \frac{\partial \psi_j}{\partial \eta} d\eta + \\
 &Sc(1 + 1.5A\eta) \bar{f}_2 \int_{\eta_e}^{\eta_{e+1}} \psi_i \psi_2 \frac{\partial \psi_j}{\partial \eta} d\eta + Sc(1 + 1.5A\eta) \bar{j}_1 \int_{\eta_e}^{\eta_{e+1}} \psi_i \psi_1 \psi_j d\eta + \\
 &Sc(1 + 1.5A\eta) \bar{j}_2 \int_{\eta_e}^{\eta_{e+1}} \psi_i \psi_2 \psi_j d\eta \\
 \tau_i^1 &= 0, \tau_i^2 = -(\psi_i \frac{\partial \psi_i}{\partial \eta})_{\eta_e}^{\eta_{e+1}}, \tau_i^3 = -(\psi_i \frac{\partial \psi_i}{\partial \eta})_{\eta_e}^{\eta_{e+1}}, \tau_i^4 = -(\psi_i \frac{\partial \psi_i}{\partial \eta})_{\eta_e}^{\eta_{e+1}}, \\
 \tau_i^5 &= -(\psi_i \frac{\partial \psi_i}{\partial \eta})_{\eta_e}^{\eta_{e+1}}
 \end{aligned}$$

Where

$$\bar{f} = \sum_{j=0}^3 f_j \psi_j, \bar{j} = \sum_{j=0}^3 j_1 \psi_j$$

4. RESULTS AND DISCUSSION

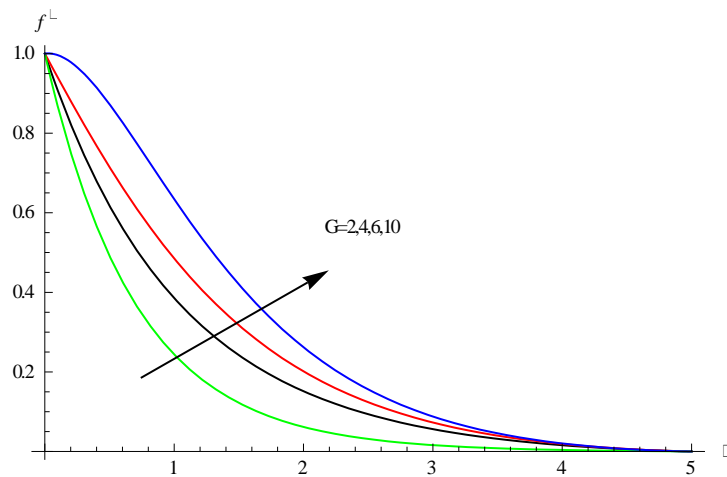
Comprehensive numerical computations were conducted for different values of the parameters and results are illustrated graphically. Selected computations are presented in Figs (2a–5d). The thickness of hydrodynamic, micro-rotation, thermal and solutal boundary layers for different values of thermal Grashof parameter (Gr) is plotted in Figs (2a-2d). It is perceived that the velocity and micro-rotation profiles are both elevated with the rising values of (Gr). However, temperature and concentration distributions are also both enhanced in the boundary layer region as the values of (Gr) increases. This is because of the reality that the inclusion of thermal Grash of number into the flow phenomenon grows as the thickness of thermal and solutal boundary layers. An increase in Gr reduces the skin friction and couple stress and increases the Nusselt and Sherwood numbers on the wall $\eta=0$.

The influence of magnetic field parameter (M) on velocity, micro-rotation, temperature and concentration profiles in the boundary layer regime is depicted in Figs (3a-3d). It is noticed from these figures that the hydrodynamic boundary layer reduces and micro-rotation boundary layer thickness enhances, whereas, thermal boundary layer thickness as well as the solutal boundary layer thickness enhances with the higher values of M . This is because of the reality that, the presence of magnetic field in an electrically conducting fluid produces a force called Lorentz force; this force acts against the flow direction causes the depreciation in velocity profiles Figs (3a&3b) and at the same time, to overcome the drag force imposed by the Lorentzian retardation the fluid has to perform extra work; this supplementary work can be converted into thermal energy which increases the thickness of thermal and solutal boundary layers in the fluid region Figs (3c&3d). Higher the Lorentz force larger the skin friction, couple stress, and smaller the Sherwood number and the Nusselt number on the wall $\eta=0$.

. Figs.4a-4d exhibits the velocity, micro-rotation, temperature and concentration with inverse Darcy parameter D^{-1} . Lesser the permeability of the porous medium smaller the velocity and the micro-rotation, larger the temperature and concentration in the flow

region. Also the skin friction and couple stress increases while the Nusselt and Sherwood numbers reduce on the wall with increase in D^{-1} on the wall $\eta=0$.

The thickness of the hydrodynamic, angular, thermal and solutal boundary layers for various values of Schmidt number (Sc) is plotted in Figs (5a-5d). The velocity of the fluid, the temperature enhances with rise in Sc and the micro-rotation, concentration reduces with Sc . The thermal boundary layer thickness is elevated, whereas, the concentration boundary layer thickness is diminished with increasing values of (Sc). Also lesser the molecular diffusivity larger the skin friction, couple stress and Sherwood number and smaller the Nusselt number on the wall $\eta=0$.



F.g.2a variation of f' with G

$$M=0.5, R=0.5, N=1, Sc=1.3, Ec=0., 01 Sr=2$$

$$Du=0.03, Q=2, A=0.2, A1=0.5, \lambda=0.5, B=0.5$$

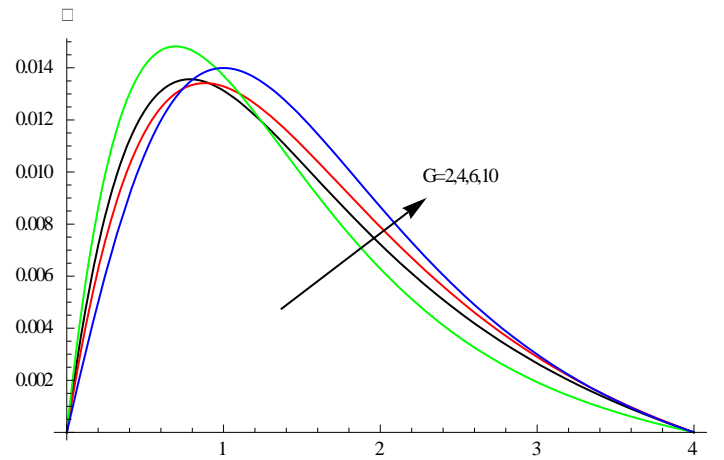


Fig.2b Variation of ω with G

$M=0.5, R=0.5, N=1, Sc=1.3, Ec=0.01, Sr=2$

$Du=0.03, Q=2, A=0.2, A1=0.5, \lambda=0.5, B=0.5$

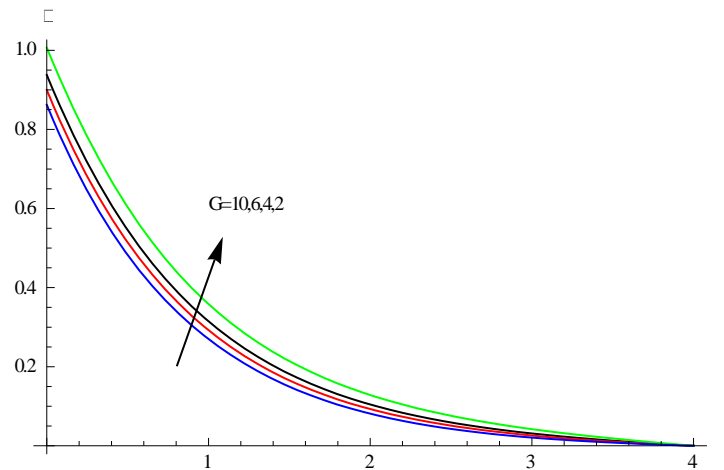


Fig.2c variation of θ with G

$M=0.5, R=0.5, N=1, Sc=1.3, Ec=0.01, Sr=2$

$Du=0.03, Q=2, A=0.2, A1=0.5, \lambda=0.5, B=0.5$

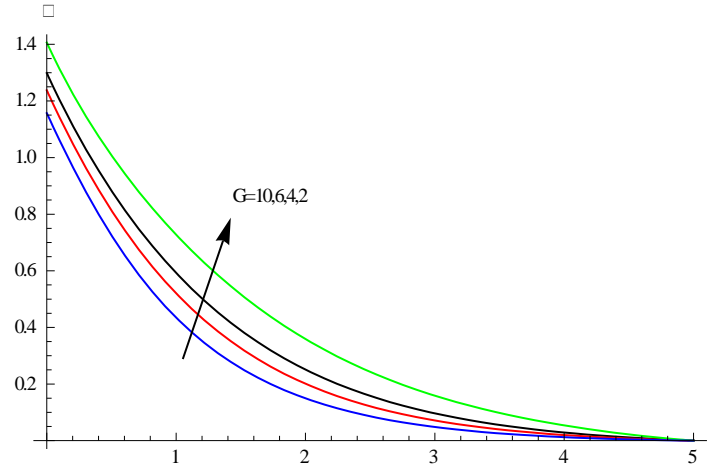


Fig.2d Variation of ϕ with G

$M=0.5, R=0.5, N=1, Sc=1.3, Ec=0.01, Sr=2$

$Du=0.03, Q=2, A=0.2, A1=0.5, \lambda=0.5, B=0.5$

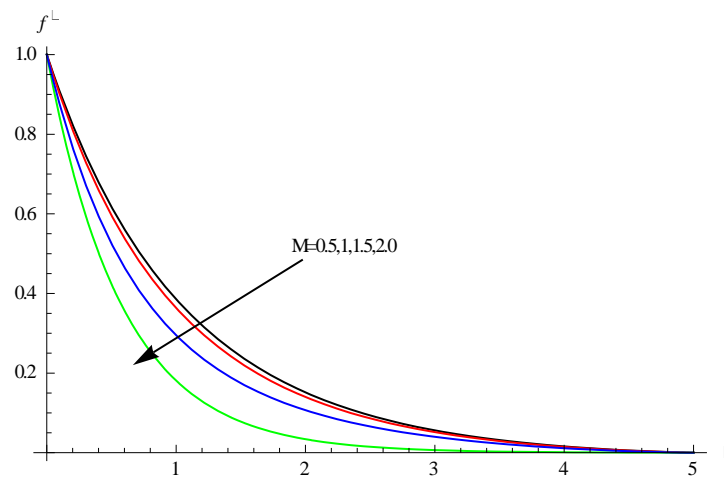


Fig.3a variation of f' with M

$G=2, R=0.5, N=1, Sc=1.3, Ec=0.01, Sr=2$

$Du=0.03, Q=2, A=0.2, A1=0.5, \lambda=0.5, B=0.5$

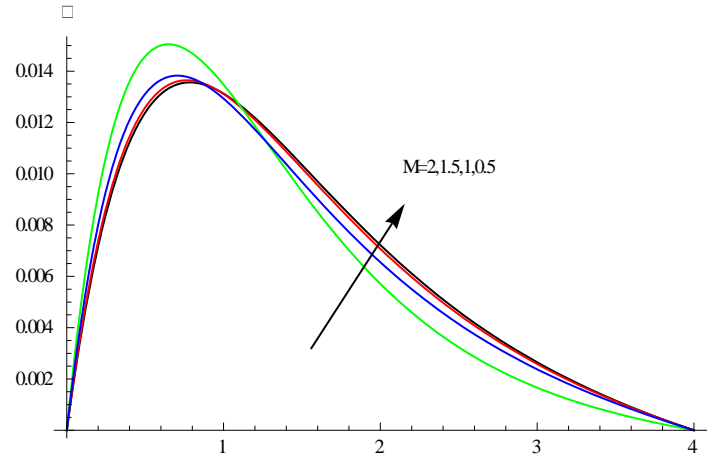


Fig.3b variation of ω with M

$G=2, R=0.5, N=1, Sc=1.3, Ec=0.01, Sr=2$

$Du=0.03, Q=2, A=0.2, A1=0.5, \lambda=0.5, B=0.5$

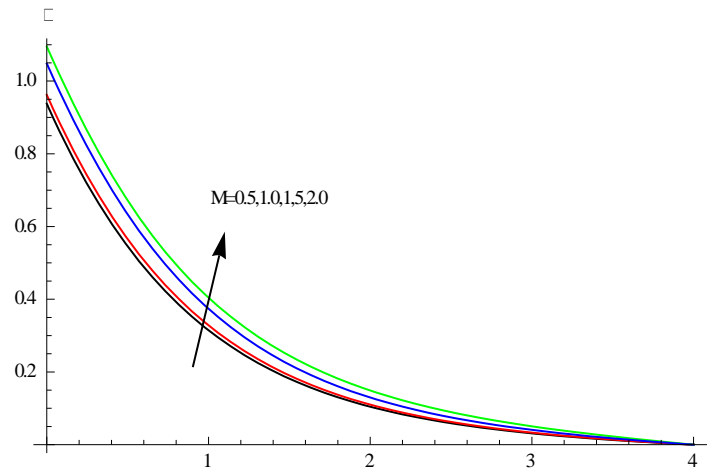


Fig.3c Variation θ with M

$G=2, R=0.5, N=1, Sc=1.3, Ec=0.01, Sr=2$

$Du=0.03, Q=2, A=0.2, A1=0.5, \lambda=0.5, B=0.5$

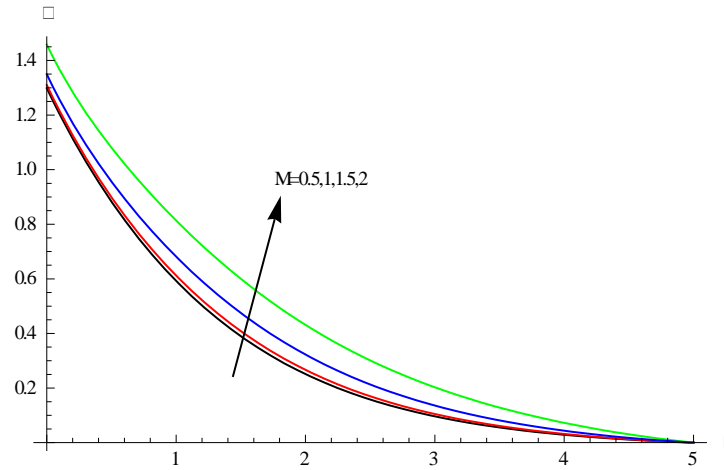


Fig.3d Variation of ϕ with M

$$G=2, R=0.5, N=1, Sc=1.3, Ec=0.01, Sr=2$$

$$Du=0.03, Q=2, A=0.2, A1=0.5, \lambda=0.5, B=0.5$$

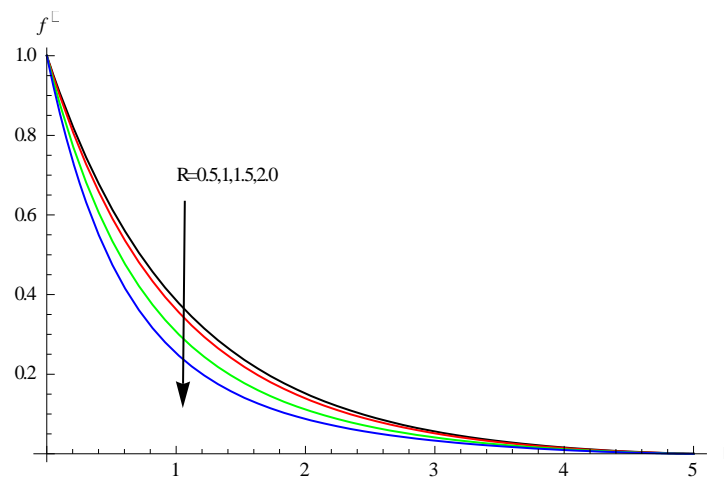


Fig.4a variation of f' with R

$$M=0.5, N=1, Sc=1.3, Ec=0.01, Sr=2$$

$$Du=0.03, Q=2, A=0.2, A1=0.5, \lambda=0.5, B=0.5$$

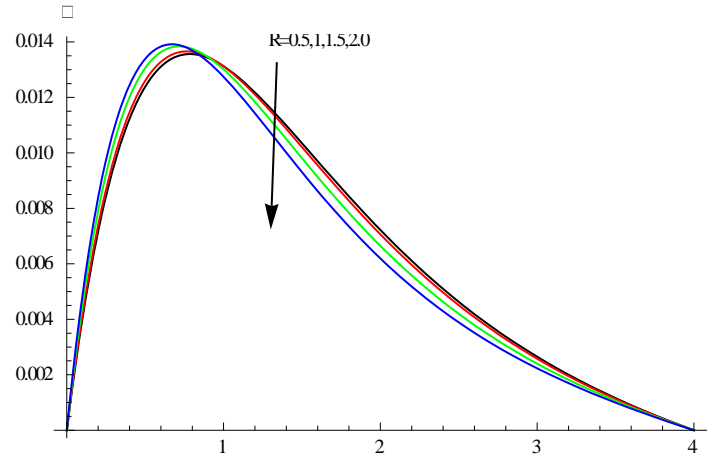


Fig.4b Variation of ω with R

$M=0.5, N=1, Sc=1.3, Ec=0.01, Sr=2$

$Du=0.03, Q=2, A=0.2, A1=0.5, \lambda=0.5, B=0.5$

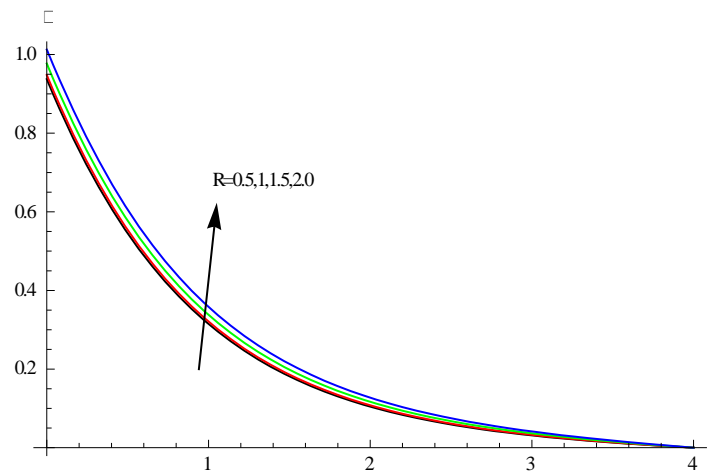


Fig.4c Variation of θ with R

$M=0.5, N=1, Sc=1.3, Ec=0.01, Sr=2$

$Du=0.03, Q=2, A=0.2, A1=0.5, \lambda=0.5, B=0.5$

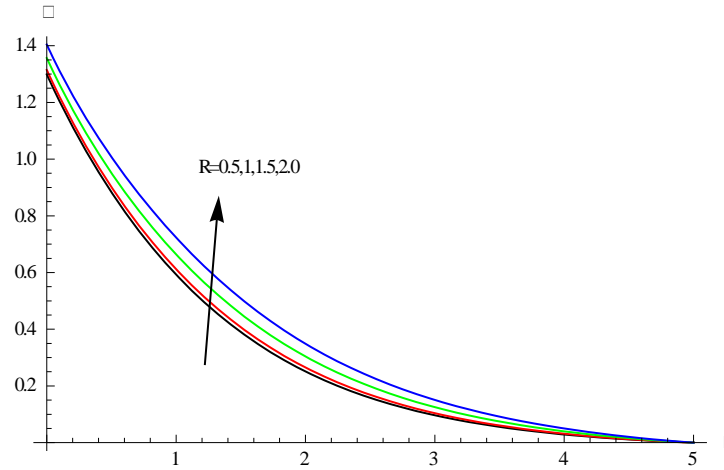


Fig.4d Variation of ϕ with R

$M=0.5, N=1, Sc=1.3, Ec=0.01, Sr=2$

$Du=0.03, Q=2, A=0.2, A1=0.5, \lambda=0.5, B=0.5$

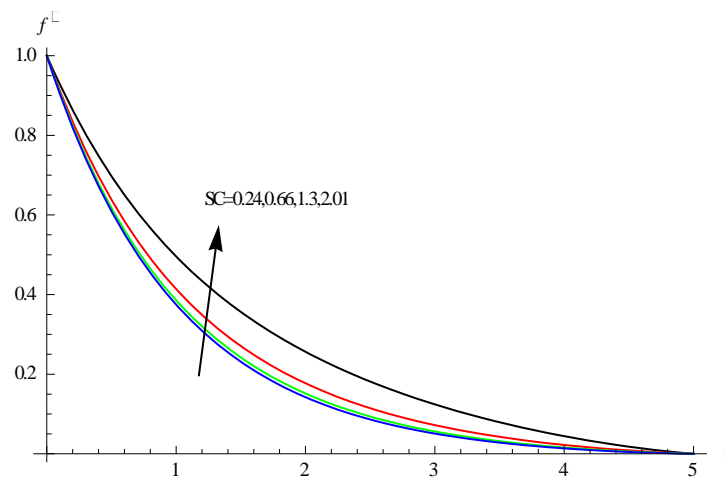


Fig.5a variation of f' with Sc

$G=2, M=0.5, R=0.5, N=1, Ec=0.01, Sr=2$

$Du=0.03, Q=2, A=0.2, A1=0.5, \lambda=0.5, B=0.5$

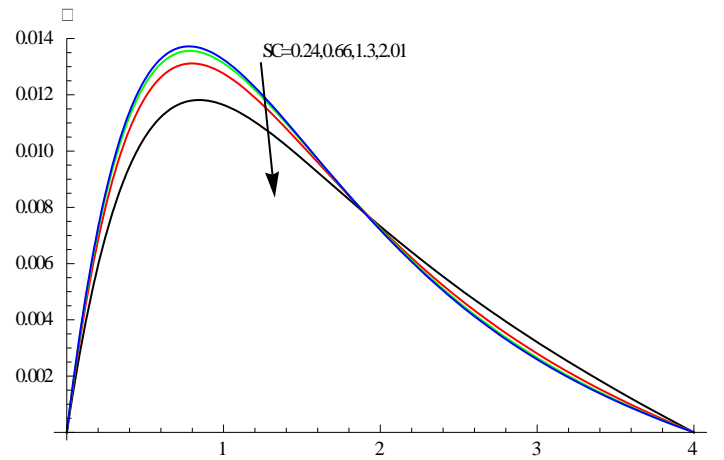


Fig.5b Variation of ωSc

$$G=2, M=0.5, R=0.5, N=1, Ec=0.01, Sr=2$$

$$Du=0.03, Q=2, A=0.2, A1=0.5, \lambda=0.5, B=0.5$$

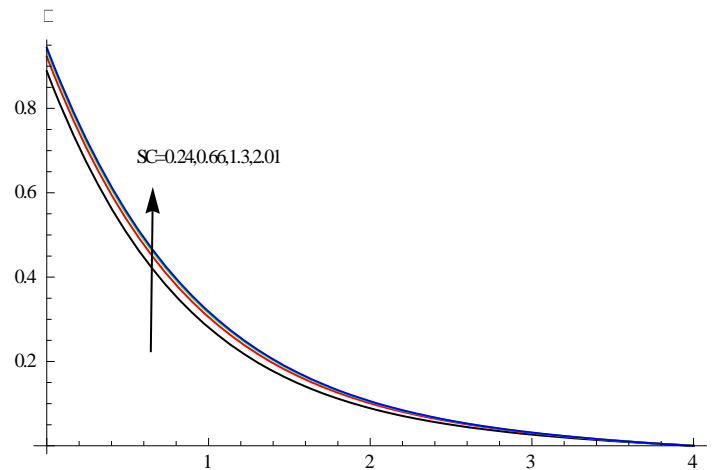


Fig.5c Variation of θSc

$$G=2, M=0.5, R=0.5, N=1, Ec=0.01, Sr=2$$

$$Du=0.03, Q=2, A=0.2, A1=0.5, \lambda=0.5, B=0.5$$

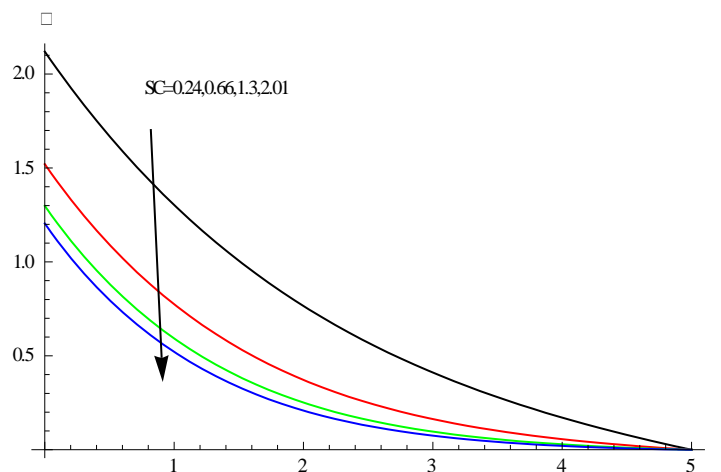


Fig.5d Variation of ϕ Sc

Comparison of local Skin-friction, Nusselt number and Sherwood number with the existing results, in the absence of heat sources ($Q=0$), Soret and Dufour effects ($Sr=Du=0$)

5. CONCLUSIONS

The combined influence of Thermo–diffusion and Diffusion–thermo effect on unsteady MHD boundary layer flow, heat and mass transfer characteristics of viscous micro polar fluid over a stretching sheet by taking suction/injection into the account is studied numerically in this paper. The important findings of this study are summarized as follows:

- Suction parameter ($fw > 0$) deteriorates the velocity, angular velocity, temperature and concentration of the fluid in the boundary layer regime.
- The velocity of the fluid diminishes, whereas, temperature of the fluid heightens with rising values of (M) and is because of the fact that the presence of magnetic field into the flow produces Lorentz force, which resist the motion of the fluid causes enhancement in the temperature.

- Increase in Soret effect (or decreasing Dufour effect) enhances the velocity, concentration profiles, whereas, depreciates the micro-rotation, temperature profiles.

- The profiles of velocity, micro-rotation, temperature and concentration of the fluid diminishes with higher values of unsteadiness parameter (A). The Skin friction, couple stress, rate of heat and mass transfer enhances with $A \leq 2$ and reduces with higher $A \geq 2.5$ at the wall $\eta = 0$.

- The temperature of the fluid rises with increasing values of Eckert number (Ec) and is because of the reality that presence of viscous dissipation produces more heat due to drag between fluid particles.

6. REFERENCES

- [1] Ali, M.E., E. Magyari : unsteady fluid and heat flow induced by a submerged stretching surface while its steady motion is slowed down gradually, Int. J. Heat mass transf. 50, pp.188-195 (2007).
- [2] Bhargava, R., Kumar, L and Takhar, H.S: Finite element solution of mixed Convection micropolar fluid driven by a porous stretching sheet, Int. J. Eng. Sci., Vol. 41, pp. 2161–2178 (2003).
- [3] Bhukta, D, G.C. Dash, S.R. Mishra : Heat and mass transfer on MHD flow of a visco elastic fluid through porous media over a shrinking sheet, Int. Scholarly Res. Notices 14, vol 11. , Article ID 572162 (2014).
- [4] Chamkha, A.J., Mohammad, R.A and Ahmad, E: Unsteady MHD natural convection from a heated vertical porous plate in a micropolar fluid with Joule heating, chemical reaction and radiation effects, Meccanica, 2010, DOI 10.1007/s11012-010-9321-0 (2010).
- [5] Chamkha, A.J. and Rashad A.M: Unsteady heat and mass transfer by MHD mixed convection flow from a rotating vertical cone with chemical reaction and Soret and

- Dufour effects, The Canadian Journal of Chemical Engineering, DOI 10.1002/cjce.21894 (2014).
- [6] Crane, L.J., Z. Angew: Flow past a stretching plate, Math. Phys, 21, pp. 645–647 (1970).
- [7] Das.K, P.R.Durai, P.K.Kundoo, Nano fluid flow over an unsteady stretching surface in presence of thermal radiation, Alexandria Eng. J.53(3), pp. 737-795 (2014).
- [8] Elbashbeshy, EMA and Bazid, MAA: Heat transfer over an unsteady stretching surface, Heat Mass Transfer, 41, pp. 1–4 (2004).
- [9] Ishak, A., Nazar, R. and Pop, I: Heat transfer over an unsteady stretching permeable surface with prescribed wall temperature, Nonlinear Anal: Real World Appl, 10, pp. 2909–13 (2009).
- [10] Ishak, A: UnsteadyMHD flow and heat transfer over a stretching plate,J. Applied Sci,10(18), pp. 2127-2131 (2010).
- [11] Kelson, N.A, A. Desseaux: Effect of surface condition on flow of micropolar fluid driven by a porous stretching sheet, Int. J. Eng. Sci. 39, pp. 1881-1897 (2001).
- [12] Lukaszewicz, G: Micropolar fluids: theory and application, Birkhäuser Basel (1999).
- [13] Makinde, O.D: On MHD Mixed Convection with Soret and Dufour Effects Past a Vertical Plate Embedded in a Porous Medium, Latin American Applied Research 41, pp. 63-68 (2011).
- [14] Mahmood, M.A.A., Waheed, S.E: MHD flow and heat transfer of a micropolar fluid over a stretching surface with heat generation (absorption) and slip velocity, J. Egypt. Math. Soc. 20(1), pp. 20-27 (2012).
- [15] Mahmood, R., Nadeem, S and Akber., N.S: Non-orthogonal stagnation point flow of a micropolar second grade fluid towards a stretching surface with heat transfer, J. Taiwan Inst.Chem. Eng., Vol. 44, pp. 586–595 (2013).
- [16] Mohammadi, M.R., Nourazar,S.S : on the insertion of a thin gas layer in micro cylindrical coquette flows involving power law liquids, Int.J.Heat Mass Transf,75, pp. 97-108 (2014).
- [17] Mohammadi, M.R., Nourazar, S.S., campo, A: Analytical solution for two- phase flow between two rotating cylinders filled with power-law liquid and a micro layer of gas,J. Mech.sci.Technol, 28(5), pp. (2014).
-

- [18] Mukhopadhyay, S: Effect of thermal radiation on unsteady mixed convection flow and heat transfer over a porous stretching surface in porous medium, *Int. J. Heat Mass Tranf.* 52, pp. 3261-3265 (2009).
- [19] Reddy, P.S and Rao, V.P: Thermo-Diffusion and Diffusion –Thermo Effects on Convective Heat and Mass Transfer through a Porous Medium in a Circular Cylindrical Annulus with Quadratic Density Temperature Variation – Finite Element Study, *Journal of Applied Fluid Mechanics*,5(4), pp. 139-144 (2012).
- [20] Rosali, H., Ishak, A. and Pop, I: Micropolar fluid flow towards a stretching/shrinking sheet in a porous medium with suction, *Int. Commun. Heat Mass Transf.* Vol. 39, pp. 826–829 (2012).
- [21] Srinivasacharya, D., Ramana murthy, J.V., Venugopalam,D., Unsteady stokes flow of micropolar fluid between two parallel porous plates, *Int. J. Eng. sci.* 39, pp. 1557-1563 (2001).
- [22] Sudarsan Reddy, P., Chamkha, AJ: Soret and Dufour effects on MHD heat and mass transfer flow of a micropolar fluid with thermophoresis particle deposition, *Journal of Naval Architecture and Marine Engineering* 13 (1), pp. 39-50 (2016).
- [23] Sudarsana Reddy, P and Chamkha, AJ: Soret and Dufour Effects on Unsteady MHD Heat and Mass Transfer over a Stretching Sheet with Thermophoresis and Non-Uniform Heat Generation/Absorption, *Journal of Applied Fluid Mechanics*, 9, pp. 2443-2455 (2016).
- [24] Tsai, R., Huang, K.H. and Huang, J.S: Flow and heat transfer over an unsteady stretching surface with non-uniform heat source, *Int. Commun. Heat Mass Transfer*, 35, pp. 1340-1343 (2008).
- [25] Tsou, F.K., Sparrow, E.M. and Goldstein, R.J: Flow and heat transfer in the boundary layer on a continuous moving surface, *Int. J. Heat Mass Transfer* 10, pp. 219–235 (1967).
- [26] Wang, CY: Liquid film on an unsteady stretching surface, *Q Appl Math*, 48, pp. 601–10 (1990).

- [27] Yacos, N.A., Ishak, A. and Pop, I: Melting heat transfer in boundary layer Stagnation point flow towards a stretching/shrinking sheet in a micropolar fluid, *Comput.Fluids*, Vol. 47, pp. 16–21 (2011).